

www.sciencemag.org/cgi/content/full/science.1197219/DC1

Supporting Online Material for **Global Trends in Wind Speed and Wave Height**

I. R. Young,* S. Zieger, A. V. Babanin

*To whom correspondence should be addressed. E-mail: ir.young@anu.edu.au

Published 24 March 2011 on *Science Express*
DOI: [10.1126/science.1197219](https://doi.org/10.1126/science.1197219)

This PDF file includes:

SOM Text
Figs. S1 to S9
Table S1
References

Supporting Online Material

Altimeter Sampling Patterns

For the present analysis, the world was divided into $2^\circ \times 2^\circ$ bins and all individual 1-second altimeter measurements assigned to a bin. For each bin, data were then considered on a monthly basis with the monthly mean, 90th percentile and 99th percentile being determined. The 90th percentile is the value which is exceeded by the upper 10% of the data. Over the 23 year time period (allowing for the break in 1990–1991), this results in approximately 260 values of each of the quantities (mean, 90th and 99th percentiles) for each $2^\circ \times 2^\circ$ bin. Zieger et al (20) calibrated the altimeter data using collocated measurements between the satellite and deep water in situ buoys. For the present analysis, it is necessary to confirm that the altimeter can accurately measure extreme wind speed and wave height conditions (i.e. 99th percentile) and that there are sufficient data points in each $2^\circ \times 2^\circ$ bin to determine such quantities on a monthly basis.

Due to the requirements of collocation in space and time between buoy and altimeter for calibration purposes, the vast majority of the calibration data of Zieger et al (20) tends to be for low to moderate sea states. As a result, some doubt arises as to the ability of the altimeter to accurately measure extreme wave heights and wind speeds. In the case of wind speed, this is particularly relevant due to the “flattening” of the transfer function relating radar cross-section and wind speed (19). In order to assess this issue, $2^\circ \times 2^\circ$ bins centred on each of the 12 deep water buoys [NODC buoys (S1)] used by Zieger et al (20) were defined. Only buoys operational for most of the 23 year time period were selected. Using the full data set (i.e. not monthly values) percentile-percentile (or Q-Q) plots were calculated for each buoy-bin combination. A typical example for buoy 46005 located at 46.1° N and 131.0° W (US Pacific coast) is shown in Fig. S1. The highest value shown on the plot is the 99th percentile. The agreement between the buoy and altimeter is excellent for the full plot, including the 99th percentile. Similar excellent agreement was obtained for each of buoys. These results indicate that the altimeter is capable of accurately measuring wind speed and wave height statistics to, at least, the 99th percentile.

This same analysis was repeated for each of the separate satellites (altimeters) which make up the combined data base. In all cases, except GEOSAT, similarly excellent agreement between buoy and altimeter was achieved. Fig. S2 shows the result for GEOSAT, averaged over all of the buoys. The GEOSAT significant wave height estimates are in excellent agreement with buoy data, however, above the 70% percentile, there is a significant overestimation of wind speed by the GEOSAT altimeter. Zieger et al (20) adopted a single transfer function to represent the relationship between radar cross-section (the quantity measured by the altimeter) and wind speed. Clearly, for the GEOSAT altimeter, this relationship performs poorly at higher wind speeds. Although it would be a relatively straight forward task to modify the relationship for GEOSAT, such a process was outside the scope of this study. Therefore, we excluded all GEOSAT wind speed data from the analysis. As a result, the analysis considered wave height over the period 1985–2008 and wind speed over the shorter period from 1991–2008 (i.e. GEOSAT excluded).

The analysis considered monthly values of mean, 90th and 99th percentiles. For these quantities to be accurately determined, there needs to be sufficient altimeter data points in each $2^\circ \times 2^\circ$ bin per month to accurately determine the values. Insufficient satellite passes may result in undersampling of extreme events. The full altimeter data set is extensive, consisting of approximately 1×10^9 observations. This represents approximately 90×10^3 observations per $2^\circ \times 2^\circ$ bin or 300 per month. To investigate whether this is sufficient observations, monthly values of mean, 90th and 99th percentile wind speed and wave height were determined for each of the buoy-bin combinations. Fig. S3 shows a typical scatter plot of each of these quantities for the same point as Fig. S1, with GEOSAT wind speed data excluded from the scatter analysis. The monthly mean, 90th and 99th percentile values appear to agree well with the buoy data (note the buoy data are based on hourly observations), scattering around the 1:1 line. Visually, there is excellent agreement for the monthly mean and 90th percentile and some tendency for the altimeter monthly 99th percentile values of both wave height and wind speed to slightly underestimate.

The bias for these monthly values can be represented as $\hat{b} = 1/n \sum_{i=1}^n (y_{alt_i} - y_{buoy_i}) / y_{buoy_i}$, where y_{buoy} and y_{alt} are the measurements of the wind speed/wave height at the buoy and altimeter, respectively (i.e. monthly mean, 90th or 99th percentile). The summation runs over all n points at a particular buoy. Averaging over all the buoys, yields values of \hat{b} for wind speed of +7% for the mean, +1% for the 90th percentile and -6% for the 99th percentile and for the wave height: +5% for the mean, +2% for the 90th percentile and -10% for the 99th percentile. A positive sign

indicates that the altimeter overestimates the monthly value. Hence, it can be concluded that the monthly analysis yields consistent results for mean and percentile values, with no clear trend indicating significant undersampling of extremes (i.e. 99th percentiles) by the altimeter. These comparisons give an indication of the relative bias when considering monthly values (means or percentiles) of less than 10%. Of course, it should be remembered that neither the buoy nor the altimeter represents the “true” value. Both are measurements, subject to instrumental error and sampling limitations. The altimeter is limited by its temporal sampling density and buoy by its spatial sampling density (i.e. a single point).

Trend Extraction

Fig. S4 shows altimeter time series of monthly mean, 90th and 99th percentile values of both wind speed and wave height at buoy locations 44011 and 46005. The data set shows a clear seasonal cycle, occasional outliers, a data gap in 1990–1991 and a visible positive trend. The aim is to determine the magnitude of any such monotonic trend and whether it is statistically significant. The determination of trend for a time series with a large seasonal signal is commonly encountered in many areas of geoscience (see Hirsch et al (*S2*) for example). In the present study a number of different techniques for the extraction of the trend were tested using synthetic data and then applied to the full data set. These techniques are briefly described below.

The most obvious approach is to adopt a simple linear regression model

$$y(t) = a_1 t + b_1 \tag{1}$$

where $y(t)$ is the value of the wind speed/wave height trend, which is a function of time, t (i.e. months). The coefficients, a_1 and b_1 can be determined by standard least squares approaches. Although this technique has been used in previous studies (*S3*, *11*, *13*, *14*), as pointed out by Sen (*S4*) it is vulnerable to gross errors and the resulting confidence limits are subject to non-normality of the parent distribution.

Some of the potential for error in the linear regression model can be removed by explicitly accounting for the seasonal signal by fitting a model of the form

$$y(t) = a_2 t + b_2 \sin(2\pi/12t + c_2) + d_2 \tag{2}$$

where the four parameters (a_2, b_2, c_2, d_2) can be determined using a least squares model. Although this approach explicitly accounts for the large seasonal signal, like all regression models with multiple parameters, it can yield spurious results when noise is present. This model was also tested with additional harmonic components (6, 4 and 3 months).

The Mann-Kendall (MK) test has been extensively applied in hydrology (*S2, S5, S6*) and in the present context by Wang and Swail (*S7*). The MK test is a non-parametric test of randomness against trend (*S4, S8, S9*). The null hypothesis of randomness, H_0 states that the data $[Y = (y_1, y_2, y_3, \dots, y_n)]$ (wave height/wind speed in this case) are a sample of n independent and identically distributed random variables. That is, there is no trend under the null hypothesis. A test statistic, S is defined as

$$S = \sum_{k=1}^{n-1} \sum_{j=k+1}^n \text{sgn}(y_j - y_k) \quad (3)$$

where

$$\text{sgn}(x) = \begin{cases} +1 & \text{if } x > 0 \\ 0 & \text{if } x = 0 \\ -1 & \text{if } x < 0 \end{cases} . \quad (4)$$

Under the assumption of H_0 , the distribution of S is symmetric and normal as $n \rightarrow \infty$ with a mean equal to zero and variance, V_S^2

$$V_S^2 = n(n-1)(2n+5)/18 \quad (5)$$

A two-sided test for trend can then be performed by comparing the following statistic

$$Z = [S - \text{sgn}(S)]/V_S \quad (6)$$

with the $\alpha/2$ percentage point of the standard normal distribution (*S2, S7*). H_0 is accepted (i.e. data are random and hence no trend) if $|Z| < Z_{\alpha/2}$. Rejection of the null hypothesis, H_0 , implies a statistically significant trend, with a positive value of Z indicating an increasing trend and a negative value a decreasing trend.

If a trend exists, Sen (*S4*) proposed that the coefficient a , as in (1), can be determined using Kendall's rank correlation (*S8*). Let t_i represent the time of observation i and for all positive differences of time between two points $(t_j - t_i)$ where $1 \leq i \leq j \leq n$ the set of slopes can be evaluated as

$$a_{ij} = (y_j - y_i)/(t_j - t_i) \quad (7)$$

The median value of the a_{ij} , yields an unbiased estimate of the trend (slope), \hat{a} .

Hirsch et al (*S2*) argue that the MK test may be too restrictive when the data are seasonal and propose a Seasonal Kendall (SK) test. The full data set, Y can be sub-divided into seasons (i.e. months)

$$Y = (Y_1, Y_2, Y_3, \dots, Y_{12}) \quad (8)$$

where

$$Y_i = (y_{i1}, y_{i2}, y_{i3}, \dots, y_{im}) \quad (9)$$

That is, (9) represents the m values associated with month i . In a similar fashion to the MK test, a statistic S_i (one for each month) can be defined as

$$S_i = \sum_{k=1}^{m_i-1} \sum_{j=k+1}^{m_i} \text{sgn}(y_{ij} - y_{ik}) \quad (10)$$

The summation statistic, $S' = \sum_{i=1}^{12} S_i$ has zero mean and variance,

$$V_{S'}^2 = \sum_{i=1}^{12} V_{S_i}^2 + \sum_{\substack{i=1 \\ i \neq l}}^{12} \sum_{l=1}^{12} \text{cov}(S_i S_l) \quad (11)$$

where $\text{cov}()$ represents the covariance. Equation (11) (*S2*) relaxes the requirement that the observations are independent and hence explicitly accounts for serial dependence in the data. Such serial dependence must exist if a trend is present in the data and is accounted for by the second term in (11). Hirsch and Slack (*S5*) discuss in detail the evaluation of the covariance term.

The standard variable, Z' is defined as

$$Z' = [S' - \text{sgn}(S')]/V_{S'} \quad (12)$$

This statistic can then be tested against the value $Z'_{\alpha/2}$, as previously, to determine statistical significance of the trend. Analogous with the MK test, the trend can be determined from the set of slopes (i.e. for month i)

$$a_{ijk} = (y_{ij} - y_{ik})/(t_{ij} - t_{ik}) \quad (13)$$

The seasonal estimator of trend magnitude is then the median of these values, \hat{a} .

In addition, to ensure that the SK test statistic and slope estimates are consistent over different seasons, a homogeneity test was proposed by van Belle and Hughes (*S6*), which assumes the data are independent. Smith et al (*S10*) modified this test to accommodate serial dependence. Following Smith et al (*S10*), let the test statistic χ_h^2 be composed of

$$\chi_h^2 = \bar{z}^T C_{\bar{z}}^{-1} \bar{z} = \chi_{trend}^2 + \chi_{residual}^2 \quad (14)$$

where \bar{z} is a column vector of SK trend statistics, $C_{\bar{z}}$ is the covariance matrix of \bar{z} , that is due to normalisation in the form of a correlation matrix, and T denotes matrix transposition. Furthermore, let χ_{trend}^2 be composed of

$$\chi_{trend}^2 = (e\bar{z})^T (eC_{\bar{z}}e^T)^{-1} (e\bar{z}) \quad (15)$$

where $e = [1, \dots, 1]$ is a ones vector of size m , and let $\chi_{\alpha, df}^2$ denote the critical value for the chi-squared distribution at the α level with df degrees of freedom. Then, a common trend over all seasons (in the same direction and magnitude) is present when testing for $\chi_{residual}^2 \leq \chi_{\alpha, m-1}^2$ and $\chi_{trend}^2 > \chi_{\alpha, 1}^2$. If $\chi_{residual}^2$ does exceed the critical value (i.e. is significant) the SK test statistic and slope estimate is misleading and the evaluation of χ_{trend}^2 is irrelevant.

Recently, Alexandrov et al (*S11*) and Alexandrov (*S12*) have proposed the use of Singular Spectrum Analysis (SSA) to extract the trend from a signal containing noise and seasonality. SSA is used extensively in the geosciences and is similar to Principal Component Analysis but is applied to a one-dimensional time series. Effectively, SSA filters the time series to leave only the long term trend. This “filtered” trend then needs to be quantified either using least squares or the MK ranking approach.

In order to test the ability of these five techniques to extract the trend from the recorded data, a series of validation tests were performed. A time series similar to the monthly values to be analysed was created. This time series was of the form: $y(t) = 3.2 + \frac{0.005}{12}t + \cos(\frac{2\pi}{12}t + 1.5) + \epsilon_t$, which has a linear trend of 0.005 units/yr, a constant offset, a seasonal component with an amplitude of 1 unit and uniformly distributed random noise, ϵ_t ranging between 0 and 0.5 units. The time series consisted of $n = 285$ monthly values and had missing data for the period 1990–1991. The magnitude of the noise is consistent with the variability observed in the recorded data and the trend to be extracted (0.005 units/yr) is generally smaller than that observed in the altimeter data. Therefore, this represents a demanding test of the analysis techniques.

Table S1 summarises the values of trend determined by the various tests, together with 95% confidence limits for the trend. All the techniques perform well, even for this quite demanding test. The SK test recovers the trend most accurately, a result confirmed with other tests with differing magnitudes of trend, noise and seasonal component. The SSA also performs well and appears to produce very small confidence limits. However, as noted above, the SSA filters the time series. The MK approach was then used to determine the trend. The confidence limits shown in Table S1 are for this filtered time series. As such, they cannot be directly compared to the other tests.

Based on these results, the SK test was adopted for further analysis. All techniques were, however, applied to the data and produced results which were very similar. The tests of statistical significance shown in Figs. 1-3 and Table 1 were determined using the approach outlined in (12) and (15), testing for the seasonal statistic Z' and for homogeneity over all seasons. In addition, these tests explicitly account for serial dependence in the data.

Statistical Variability

Figs. 1-3 and Table 1 show variability in the trend determined from neighbouring $2^\circ \times 2^\circ$ bins or between different buoys in the same geographic region (eg. Buoys 46005 and 46006, both in the North Pacific, yield trends for the 99th percentile wind speed of 8.89 cm/s/yr and 12.70 cm/s/yr, respectively, see Table 1). To investigate the potential reason for such variability, a Monte-Carlo simulation was performed. As noted in Fig. S3, there is sampling variability in the measured values of monthly statistics, whether determined from buoy or altimeter. Based on an examination of values of \hat{b} , it was assumed that the variability of the 99th percentile values could be approximated by a normal distribution with standard deviations, σ of 0.7m and 0.9m/s for the wave height and wind speed, respectively. Note that for a normal distribution, 68.2% of values lie within $\pm\sigma$. In the Monte-Carlo simulation, the observed value for the 99th percentile was taken as the mean of the distribution. A total of 10,000 realisations of each value in the time series were generated, conforming to the assumed normal distribution. The SK trend estimate was applied to each realisation of the time series. The resulting values of trend followed an approximate normal distribution with 95% confidence limits of ± 2.64 cm/s/yr for wind speed and ± 1.95 cm/s for wave height. This level of variability is consistent with Figs. 1-3 and Table 1.

Changes in Sampling Density and Instrumentation

In the later years of the 23 year data set, there were multiple satellites in orbit. As a result, the data density was greater in these later years. An increase in sampling density could result in a greater number of short time and space scale events being observed. In order to determine if this has an impact on the results, the data were randomly decimated such that for each $2^\circ \times 2^\circ$ bin a constant number of observations were achieved per month throughout the full period of the data set. The monthly mean and percentile values were again calculated. Initially, these values were compared with the buoy estimates, as in Fig. S3 and the mean bias, \hat{b} calculated for the decimated altimeter data corresponding to each buoy location. The average value of \hat{b} for all 12 buoys was almost unchanged, both in sign and magnitude compared to the undecimated result. The decimated analysis yields values of \hat{b} (undecimated comparison in parenthesis) for wind speed of +7% (+7%) for the mean, +1% (+1%) for the 90th percentile and -5% (-6%) for the 99th percentile and for wave height: +5% (+5%) for the mean, +3% (+2%) for the 90th percentile and -10% (-10%) for the 99th percentile. The SK trend process was also repeated for the full globe with this decimated data. The resulting colour filled contour plots for the 99th percentile values are shown in Fig. S5. Comparisons showed almost identical results for both the mean and 90th percentile (not shown here). The 99th percentile shows (compare Fig. 3 with Fig. S5) a slightly weaker trend for the decimated data. The average difference (i.e. undecimated percentage trend minus decimated percentage trend averaged over the whole globe) for the SK method are – wind speed: 0.00% per year for the mean, +0.03% per year for the 90th percentile and +0.11% per year for the 99th percentile and wave height: 0.00% per year for the mean, +0.03% per year for the 90th percentile and +0.17% per year for the 99th percentile. These results indicate that the increasing data density has some effect at the 99th percentile level. However, the global positive trend observed for the full data set is still clearly present and the bias introduced by changes in the sampling density is typically within the 95% confidence limits described above. As a result, it can be concluded that the variation in data density throughout the full period of the time series does not significantly bias the results.

Altimeter Trend Validation

As noted, the wind speed and wave height trends obtained from the altimeter data are consistent with buoy data (see Table 1). However, as the altimeter data were originally calibrated using buoy data, this does not represent a completely independent validation of the results. Further validation evidence was sought by comparison with numerical model results. For this purpose, NCEP/NCAR reanalysis monthly mean wind speed data were used (25) (<http://www.esrl.noaa.gov/psd/data/gridded/data.ncep.reanalysis.derived.surface.html>). The NCEP/NCAR Reanalysis 1 product incorporates data assimilation from instrumentation systems independent of those used here. The monthly mean data were obtained from 6 hourly results. With 6 hourly data, it is not possible to form accurate percentile values. However, the SK test was applied to the monthly mean results to form trends for the 1991–2008 period (as for the altimeter data), the results being shown in Fig. S6. Fig. 1 and Fig. S6 (ie. altimeter and model) show many similar qualitative features. Both model and altimeter results show a strong positive trend in the equatorial Pacific with smaller regions of negative trend east of New Guinea and east of Japan. Both data sets also show a stronger positive trend in the south Pacific than in the north Pacific. Within the Indian Ocean, both data sets reveal a band of stronger positive trend stretching from Indonesia towards Madagascar. Overall, the altimeter shows slightly stronger positive trends than the model results.

These model results, together with the consistent buoy trends support the global values determined from the altimeter data set.

Summary

The above analyses have carefully investigated the ability to accurately extract trends from the altimeter data set. In particular, the analysis has investigated:

- Methods to extract relatively small trends in a data set with a large season signal and noise.
- Methods to determine if measured trends are statistically significant including accounting for serial dependence and homogeneity across months (seasons).

- The ability of the altimeter to accurately measure wind speed and wave height up to the 99th percentile.
- The reliability of each separate altimeter in measuring such extreme conditions.
- Any impact on measured values of monthly 90th and 99th percentile values due to the sampling density of the altimeter.
- The impact of an increase in the sampling density of observations in the latter years of the time series.
- The sampling variability one could expect in derived values of trend, as a result of sampling variability in monthly values.
- Whether trends extracted from the altimeter data base are consistent with buoy and numerical model results.

This extensive analysis concludes that the observed trends are a reliable and unbiased estimate of changes in the wind speed and wave height climate over the period of the measured time series.

Data source

Altimeter missions from which data have been used in the present analysis were sourced as follows:

- GEOSAT – available on CD from:
<http://www.nodc.noaa.gov/General/CDR-detdesc/geosatj3.html>
- ENVISAT, ERS1, and ERS2 – available on request from: <http://eopi.esa.int>
- TOPEX – available from:
ftp://podaac.jpl.nasa.gov/pub/sea_surface_height/topex_poseidon/mgdrb/data/
- JASON1 – available from:
ftp://podaac.jpl.nasa.gov/pub/sea_surface_height/jason/gdr_b/data/
- GFO – available from: ftp://gfo:cal_val!@eagle.grdl.noaa.gov/gdr/poe/noaa/

References and Notes

- S1. D. Evans, C. L. Conrad, F. M. Paul, Handbook of Automated Data Quality Control Checks and Procedures of the National Data Buoy Center, *Technical Document 03-02*, NOAA National Data Buoy Center (2003).
- S2. R. M. Hirsch, J. R. Slack, R. A. Smith, *Water Resour. Res.* **18**, 107 (1982).
- S3. D. K. Woolf, P. D. Cotton, P. G. Challenor, *Phil. Trans. R. Soc. Lond. A* **361**, 27 (2003).
- S4. P. K. Sen, *J. Amer. Statist. Assoc.* **63**, 1379 (1968).
- S5. R. M. Hirsch, J. R. Slack, *Water Resour. Res.* **20**, 727 (1984).
- S6. G. Van Belle, J. P. Hughes, *Water Resour. Res.* **20**, 127 (1984).
- S7. X. L. Wang, V. R. Swail, *J. Clim.* **14**, 2204 (2001).
- S8. M. Kendall, *Rank Correlation Methods* (Griffin, London, 1955).
- S9. H. B. Mann, *Econometrica* **13**, 245 (1945).
- S10. E. P. Smith, S. Rheem, G. I. Holtzman, *Multivariate Environmental Statistics*, G. P. Patil, C. R. Rao, eds. (North-Holland, 1993), pp. 489–508.
- S11. T. Alexandrov, S. Bianconicini, E. B. Dagum, P. Mass, T. S. McElroy, A review of modern approaches to the problem of trend extraction, *Tech. Report RRS2008/03*, US Census Bureau, Washington, DC (2008).
- S12. T. Alexandrov, *Revstat Stat. J.* **7**, 1 (2009).

Table S1: Test results for trend extraction algorithms. The target value for the trend in this test is 0.5×10^{-2} units/yr. *SSA was used to “filter” the time series. The trend of the filtered time series was then determined using the MK test. The confidence limits are for this filtered time series.

Analysis Technique	Trend [units/yr $\times 10^{-2}$] Target value = 0.5×10^{-2} units/yr	95% Confidence Limits [units/yr $\times 10^{-2}$]
Linear regression (1)	0.57	-0.70 - 1.83
Linear plus seasonal (2)	0.48	0.23 - 0.74
Mann-Kendall test (7)	0.53	-0.66 - 1.73
Seasonal Kendall test (13)	0.50	0.25 - 0.77
Singular Spectrum Analysis* (SSA)	0.48	0.43 - 0.53

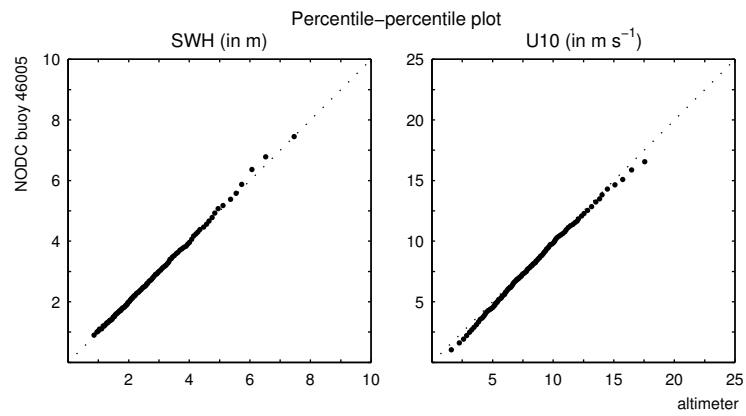


Figure S1: Percentile-percentile (Q-Q) plots between altimeter (horizontal axis) and buoy (vertical axis) for buoy 46005. Significant wave height is shown in the left panel and wind speed in the right panel.

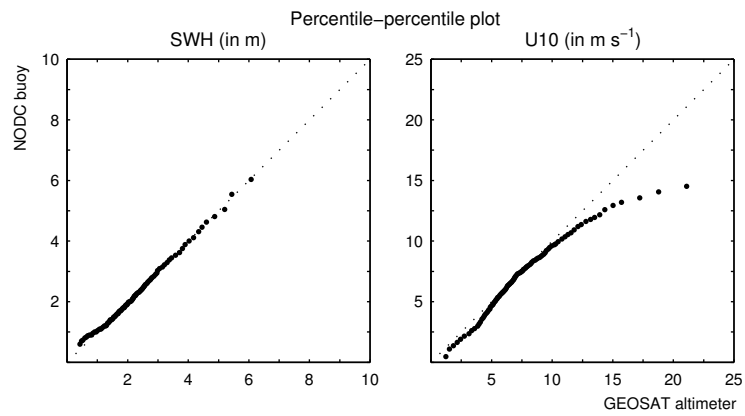


Figure S2: Percentile-percentile (Q-Q) plots for the GEOSAT altimeter. Altimeter values are shown on the horizontal axis and buoy values on the vertical axis. The data is taken from all available buoy locations. Significant wave height is shown in the left panel and wind speed in the right panel.

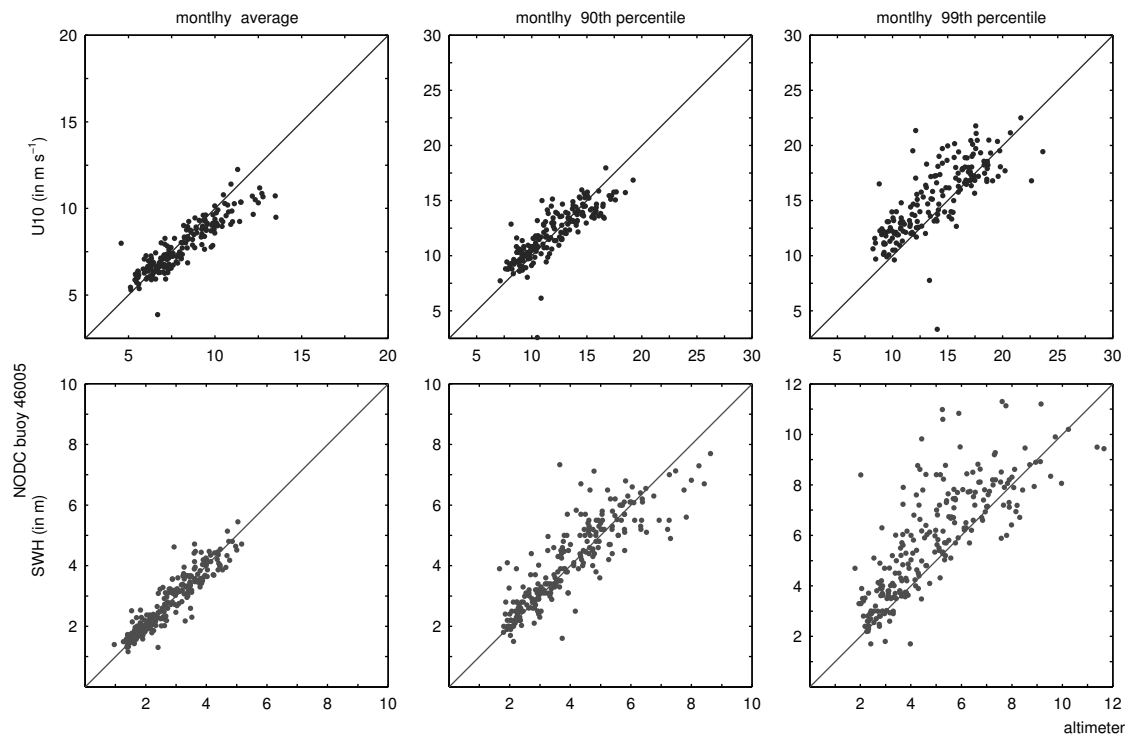


Figure S3: Scatter plot of monthly mean, 90th and 99th percentile values of wind speed (top panels) and wave height (bottom panels) comparing altimeter and buoy. Results are shown for buoy 46005.

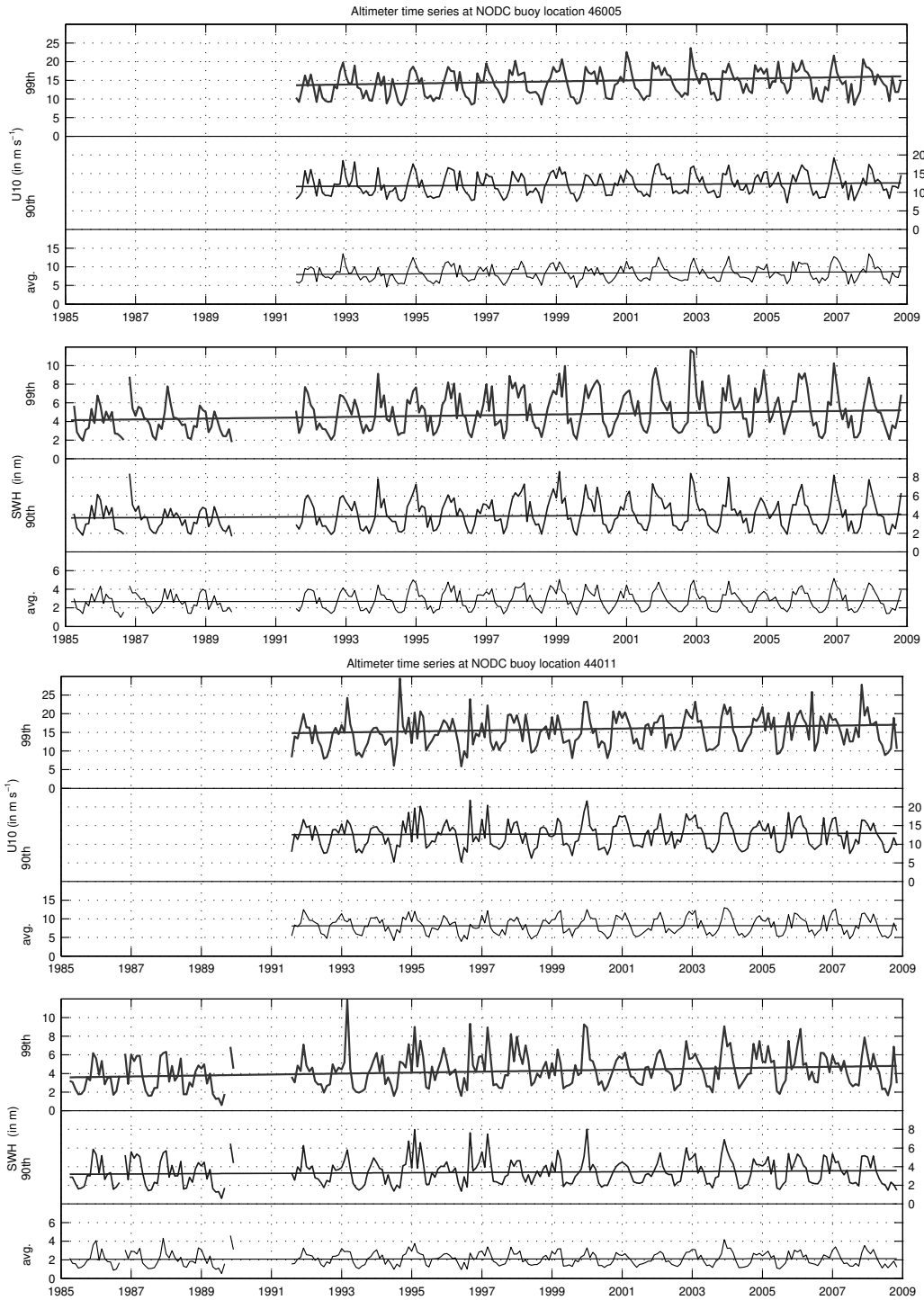


Figure S4: Altimeter time series of monthly values of mean, 90th and 99th percentile values of wind speed and wave height for (top panels) location 131.0°W, 46.1°N (NODC Buoy 46005) and (bottom panels) location 66.6°W, 41.1°N (NODC Buoy 44011). The trend for each time series, as calculated by the SK test method is also shown.

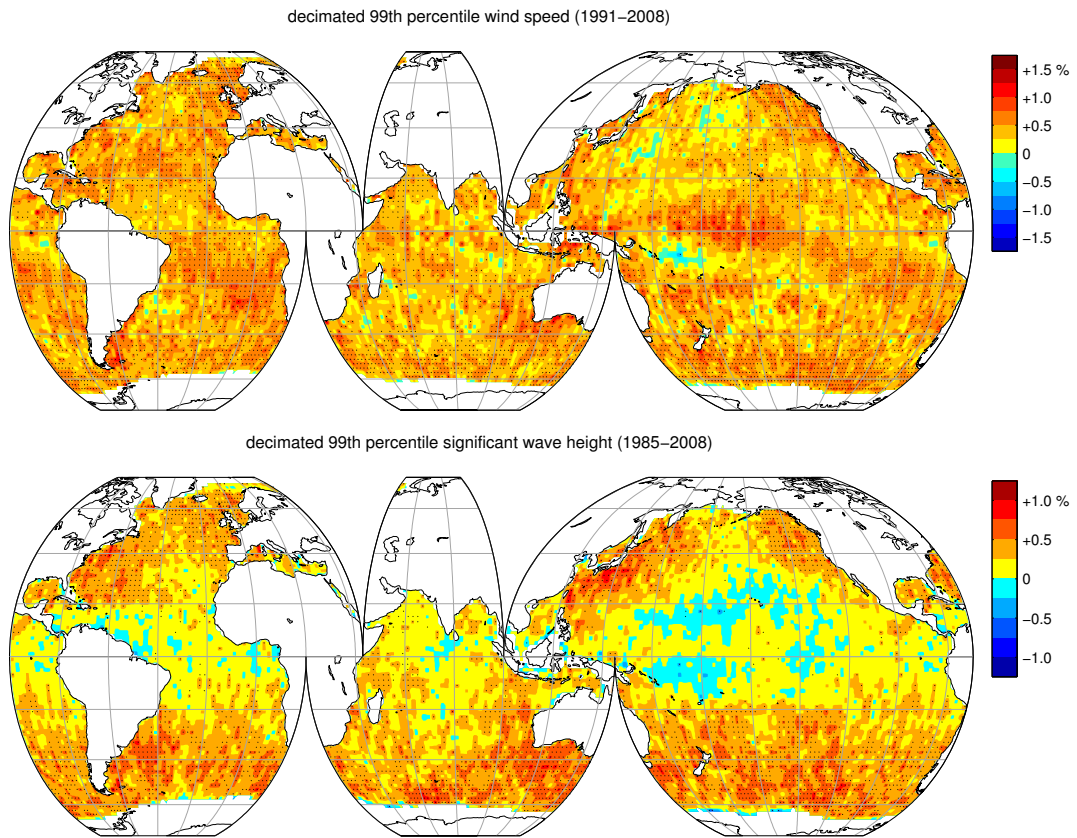


Figure S5: Colour contour plots of the 99th percentile trend (% per annum). Data have been decimated such that there is a constant sampling density throughout the 23 year duration of the data. Wind speed is shown at the top and wave height at the bottom. Points which are statistically significant according to the SK test are shown with dots.

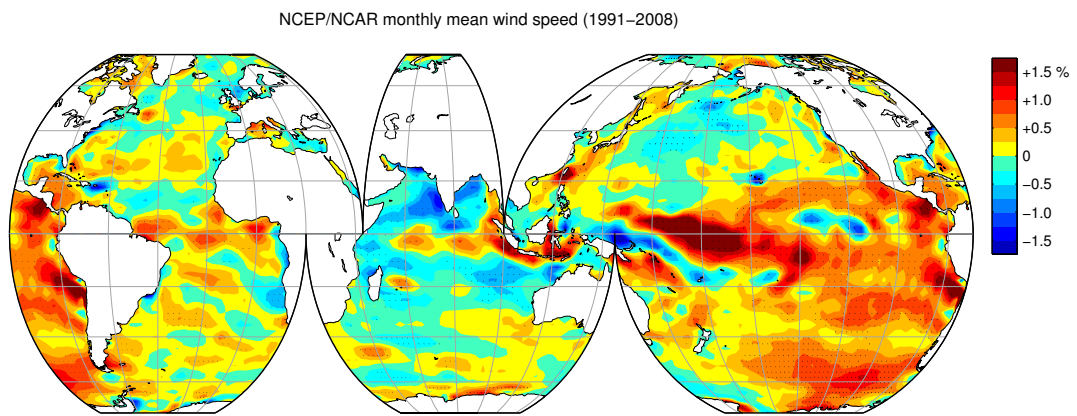


Figure S6: Colour contour plot of mean monthly wind speed trend (% per annum) from the NCEP/NCAR reanalysis data (25). Points which are statistically significant according to the SK test are shown with dots. This figure can be directly compared with Fig. 1.

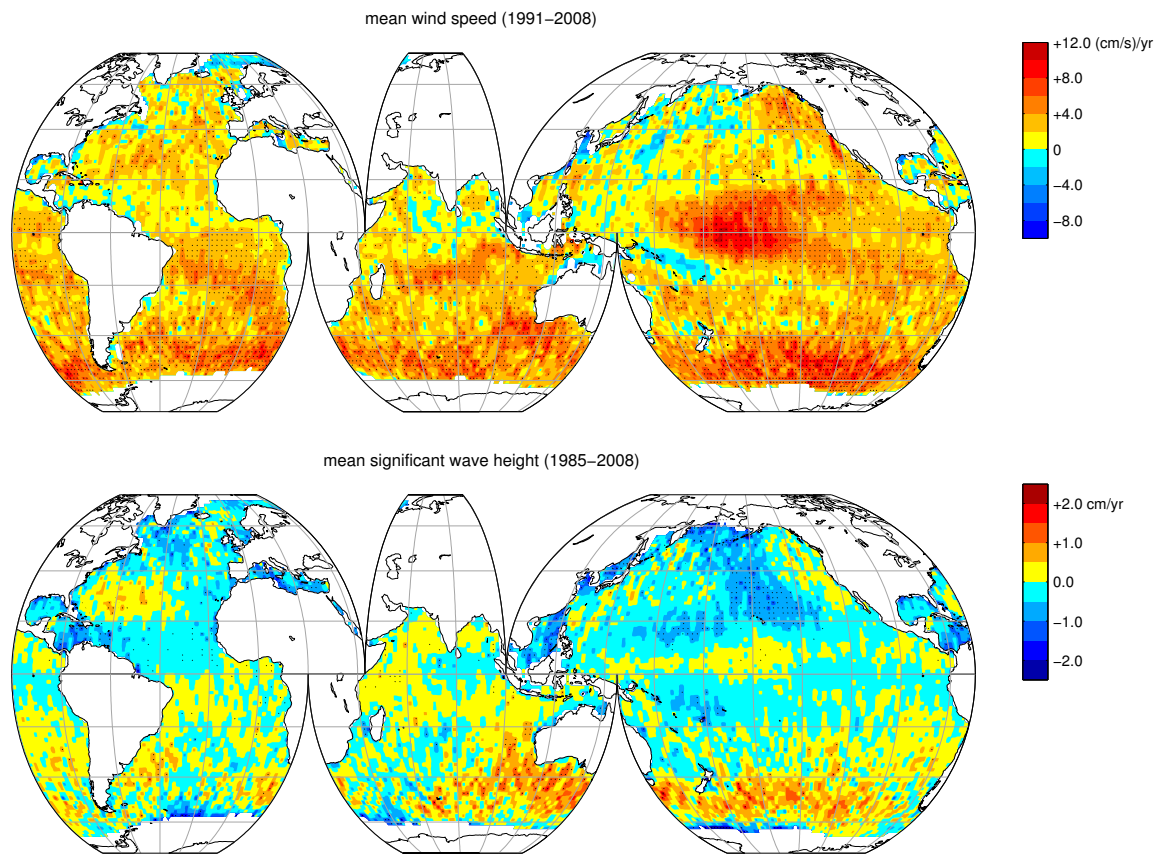


Figure S7: Colour contour plots of mean trend (absolute values). Wind speed is shown at the top and wave height at the bottom. Points which are statistically significant according to the SK test are shown with dots. This figure can be directly compared with Fig. 1.

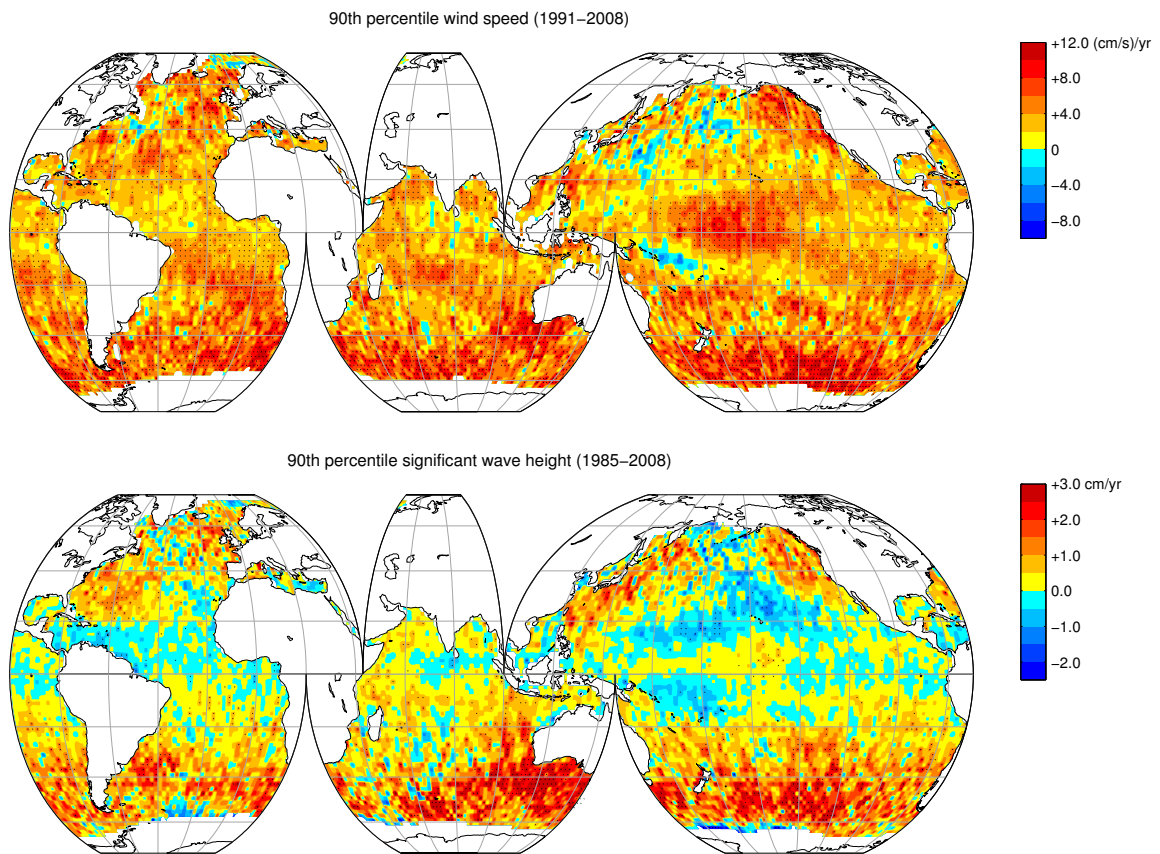


Figure S8: Colour contour plots of the 90th percentile trend (absolute values). Wind speed is shown at the top and wave height at the bottom. Points which are statistically significant according to the SK test are shown with dots. This figure can be directly compared with Fig. 2.

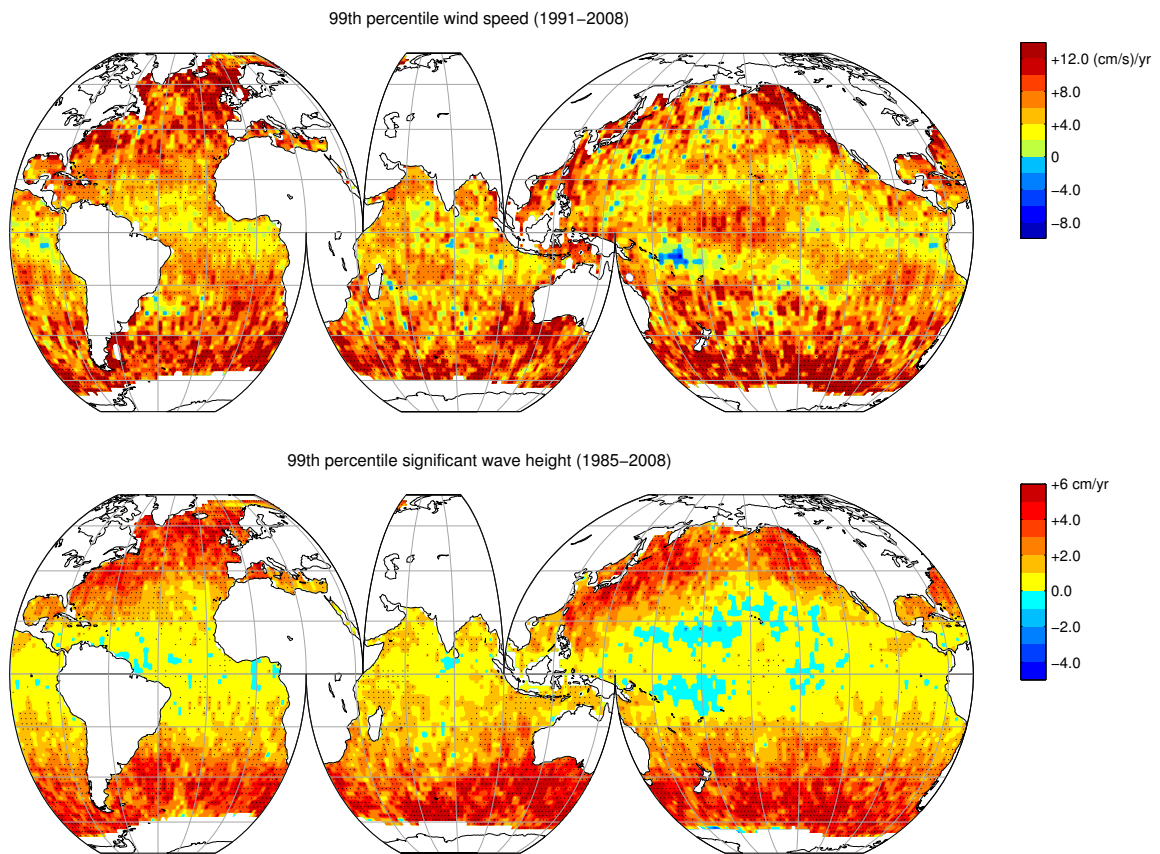


Figure S9: Colour contour plots of the 99th percentile trend (absolute values). Wind speed is shown at the top and wave height at the bottom. Points which are statistically significant according to the SK test are shown with dots. This figure can be directly compared with Fig. 3.